

Separation Performance of Si-CHA Zeolite Membrane for a Binary H₂/CH₄ Mixture and Ternary and Quaternary Mixtures Containing Impurities

Tangyin Wu, Chaojiu Shu, Shuai Liu, Boshen Xu, Shenglai Zhong,* and Rongfei Zhou*



Cite This: <https://dx.doi.org/10.1021/acs.energyfuels.0c01720>



Read Online

ACCESS |

Metrics & More

Article Recommendations

Supporting Information

ABSTRACT: The separation of H₂/CH₄ mixtures is very common in the natural gas and petrochemical industries. There are some higher C₂–C₄ hydrocarbons and water vapor that are used as impurity gases. Si-CHA zeolite membranes display a high H₂ permeance of 1.44×10^{-6} mol/(m² s Pa) (permeability of 10800 barrers) and H₂/CH₄ selectivity of 85 for an equimolar H₂/CH₄ mixture at 298 K and 0.2 MPa pressure drop. A third gas decreased H₂ permeance and H₂/CH₄ selectivity of the membrane. Hydrogen permeance was reduced in an order similar to the adsorption amount in zeolite: H₂O > C₃H₈ > n-butane > ethane. The effects of temperature, pressure, and feed concentration were studied on separation performances of the membrane in the binary and ternary mixtures. A simple model was built up to predict the reduction of permeance and selectivity when multi impurities were contained, and the predicted value agreed well with the tested one. A stable performance was obtained within several hours in all the tests. The separation performance of the membrane was recovered to the original level when the impurity gas was removed.

1. INTRODUCTION

Hydrogen, as a carrier of clean energy, has become a promising energy to reduce climate change and air pollution mainly due to the rapid development of fuel cells.^{1,2} Most of hydrogen is currently produced from the reforming and cracking processes of petroleum and water–gas shift reaction, while some hydrogen is produced from biomass gas.³ In the former case, hydrogen is always mixed with light hydrocarbons (methane, ethane, propane, etc.) and other impurities. For example, hydrogen is formed as a main byproduct in the ethylene industry when naphtha is cracked to smaller C₁–C₄ hydrocarbons. The light composition with the main body of hydrogen and methane is easily separated from heavier composition C₂–C₄ hydrocarbons by distillation. Hydrogen can be further purified from methane by pressure swing adsorption, low temperature distillation, and membrane separation.⁴ Membrane separation has the advantages of high separation efficiency, low energy consumption, and continuous operation compared with other two methods, and it is promising for molecular separations^{5–9} including hydrogen purification.^{5,6,9}

Crystalline zeolite and metal organic framework (MOF) membranes can separate molecules with high flux and high selectivity by molecular sieving and preferential adsorption mechanisms. Huang et al.¹⁰ developed a new type of two-layered ZIF-8@GO membrane with a H₂/CH₄ separation factor of 139.1 and H₂ permeance of 1.3×10^{-7} mol/(m² s Pa) at 523 K. Caro et al.¹¹ prepared a high c-oriented NH₂-MIL-125 MOF film on porous α -alumina substrate; the membrane showed a H₂/CH₄ ideal selectivity of 11.2 and H₂ permeance of 4.375×10^{-8} mol/(m² s Pa) at 298 K and 0.1 MPa. Lin et al.¹² reported that a DDR zeolite membrane after chemical

vapor deposition modification had a H₂ permeance of 1.2×10^{-8} mol/(m² s Pa) and H₂/CO selectivity of 11.

A zeolite CHA framework has an 8-member-ring, straight, and 3D pore structure with a pore window size of 3.8 Å × 3.8 Å. It is a promising membrane material for distinguishing hydrogen (kinetic diameter of 2.8 Å) from methane (kinetic diameter of 3.8 Å) or higher hydrocarbons by size difference.¹³ There were some reports^{14–19} to develop CHA zeolite membranes such as chabazite, SSZ-13, and Si-CHA for CO₂ separation from N₂ and CH₄. But, the literature for H₂/CH₄ separation using CHA zeolite membranes is very scarce.²⁰

The current membranes^{15,20–24} normally display relatively low H₂ permeances in the order of 10^{-8} – 10^{-7} mol/(m² s Pa) when H₂/CH₄ selectivities are higher than 30 in a binary mixture. A highly H₂ permeable and selective membrane is necessary to reduce the cost of inorganic membrane modules.²⁵ Meanwhile, impurity gases such as C₂–C₄ hydrocarbons and water vapor are normally contained in H₂/CH₄ mixtures when they were derived from the ethylene industry and purge gas. There were no reports on the influences of these impurity gases on separation performance and the stability of the membrane for H₂/CH₄ mixtures containing impurities.

There are some references^{26–33} that investigate the effects of impurity gases of C₂–C₄ hydrocarbons and water vapor on the separation performances of zeolite membranes in terms of

Received: May 29, 2020

Revised: July 20, 2020

Published: August 4, 2020

CO_2/CH_4 separations. Li et al.³⁰ reported that CO_2 permeance and CO_2/CH_4 selectivity of SAPO-34 membrane decreased to a larger extent by adding only 0.1% *n*-butane than that by adding 1% ethane and propane. The stability period for the stable separation performance of SAPO-34 membrane by adding propane was the longest among C2–C4 normal alkanes. The stability period was shortened by factors of 0.75 when a high-silica SSZ-13 membrane³³ was used.

For H_2/N_2 separation²⁶ through SSZ-13 and SAPO-34 membranes, the addition of a low concentration of propane or *n*-butane decreased N_2 permeance more than H_2 permeance, and thus, H_2/N_2 selectivity increased from 4.1 to 7.2. The impurities of normal alkanes such as *n*-butane and propane swelled the 10-member-ring MFI zeolite membrane²⁹ (5.5 Å) and decreased the size of defects. As a result, $\text{H}_2/\text{n-C}_4\text{H}_8$ and $\text{H}_2/\text{C}_3\text{H}_8$ selectivities increased. The effects of impurity gases such as higher hydrocarbons were complicated and highly dependent on membrane microstructures and separation pairs. Water vapor decreased CO_2/CH_4 and CO_2/N_2 separation performances using low-silica CHA (chabazite) membranes.²⁷ Most of the MOF membranes^{28,31,32} were sensitive to water vapor. High-silica CHA (SSZ-13) and pure-silica CHA (Si-CHA) zeolite membranes²⁷ displayed a higher tolerance to water vapor for CO_2 separations.

In this current study, we have reported H_2/CH_4 separations using a novel Si-CHA zeolite membrane. The best membrane showed H_2 permeance of 1.44×10^{-6} mol/(m^2 s Pa), and H_2/CH_4 selectivity was higher than 70 for an equimolar binary H_2/CH_4 mixture. The influences of C2–C4 alkanes and water vapor on the separation performance of Si-CHA zeolite membranes for ternary and quaternary mixtures were initially investigated. The stabilizing period for all the ternary and quaternary mixtures was less than 6 h. Meanwhile, the membrane displayed good stability in wet mixtures.

2. EXPERIMENTAL SECTION

2.1. Synthesis of Si-CHA Zeolite Membranes. Si-CHA zeolite membranes were synthesized using a novel fluoride-free all-silica gel, as described in our latest paper.³⁴ The synthesis using our diluted fluoride-free gel was more environment-friendly and reproducible than that using paste-like and HF-containing gel.³⁵ The α -alumina tubes (200 nm average pore size) from Inopor Co. were cut into 6 cm long pieces and were washed with boiling DI water. The internal surface of the dried support was coated with seeds by rubbing. The membrane gel was prepared by mixing *N,N,N*-trimethyl-1-adamantammonium hydroxide (TMAdaOH), DI water, sodium hydroxide (99%, Aldrich), and colloidal silica (40% in water, Aldrich). The alumina-free solution had a mole ratio of 10.0 SiO_2 /2.0 Na_2O /1.0 TMAdaOH/1200 H_2O . The seeded support was placed in an autoclave containing membrane gel. The hydrothermal treatment was carried out in an oven at 443 K for 3–4 d. The resulting membranes were washed and calcined at 673 K for 6 h with change rate of 1 K/min.

2.2. Characterization and Separation Performance. The structures of crystals and membranes were confirmed by X-ray diffraction (XRD, Ultima IV) with Cu $\text{K}\alpha$ radiation at 2θ from 5° to 45° and a step size of 0.05° . The tubular Si-CHA zeolite membranes were cut into several slips with a length of about 20 mm, and the width of about 3 mm. The inner surfaces of the four slips connected by the adhesive tape were exposed for the X-ray scans. The morphologies of the crystals and membranes were determined by field emission scanning electron microscopy (FE-SEM, Hitachi S-4800) at acceleration voltages of 5–10 kV. Adsorption isotherms for H_2 , CH_4 , C_2H_6 , C_3H_8 , and $\text{n-C}_4\text{H}_{10}$ were measured on Si-CHA crystals using adsorption apparatus (ASAP2020M, Micromeritics).

Before adsorption measurements, the samples were calcined at 773 K for 6 h and degassed in a vacuum at 493 K overnight.

Single-gas permeances and mixed-gas separation were carried out using the two systems described previously.¹⁷ Single-gas permeances for H_2 , CO_2 , N_2 , CH_4 , C_2H_6 , and C_3H_8 were measured using a dead-end system. Mixed-gas separations were measured as functions of pressure and temperature using the flow system for an equimolar H_2/CH_4 binary mixture. Separation performances in other ternary mixtures ($\text{H}_2/\text{CH}_4/\text{C}_2\text{H}_6$, $\text{H}_2/\text{CH}_4/\text{C}_3\text{H}_8/\text{H}_2/\text{CH}_4/\text{n-C}_4\text{H}_{10}$, and $\text{H}_2/\text{CH}_4/\text{H}_2\text{O}$) and quaternary mixtures ($\text{H}_2/\text{CH}_4/\text{C}_3\text{H}_8/\text{C}_2\text{H}_6$ and $\text{H}_2/\text{CH}_4/\text{H}_2\text{O}/\text{C}_3\text{H}_8$) through the typical Si-CHA zeolite membranes were tested as a function of test time. For some cases with water vapor, the gas stream of mixed H_2 and CH_4 was introduced in a water trap to take the water vapor into the mixture. The content of water vapor was tuned by controlling the temperature of bath as described in our previous study.³⁶ No sweep gas was used for all the tests. The flux of membrane was measured with bubble flow meters. The composition in the permeate and retentate sides was analyzed by a gas chromatograph (Shimadzu GC-14C) equipped with a TCD and a Hayesep D column at 373 K. Most of the tests were carried out using a total feed flow rate up to 4.0 standard liter per minute (SLPM) to minimize the concentration polarization. The permeate pressure was kept at 0.103 MPa (absolute pressure). The total feed flow rate decreased to 1.0 SLPM for some long-term tests to reduce the consumption of gas. The ideal selectivity is the ratio of the single-gas permeance. The binary separation selectivity is the ratio of the permeance for binary mixtures. A log-mean pressure drop was used in the calculation of permeance as described in our previous study.²⁰ Separation index is defined as CO_2 permeance times (selectivity – 1) times permeate pressure. It is another parameter to comprehensively evaluate the membrane performance as used in the literature.³⁷

In a ternary or quaternary mixture, the permeance of each composition was obtained by the same method as that in binary mixture. The selectivity of H_2 over another gas was the ratio of their permeances. Please note that only a trace of ethane in the permeate side was detected when 1–5 mol % impurity gas (C2–C4 or water vapor) was added in the gas mixture. The content of propane, *n*-butane, and water in the permeate side was out of the detection limit of our GC. It showed that the typical membranes had good quality with a very low concentration of defects.

The selectivity and permeance are reduced by adding one or two impurity compositions. The tested reduction rate was obtained by comparing the permeance or selectivity before and after the addition of impurity gases according to the following eqs 1 and 2. The predicted reduction in quaternary mixture was obtained from the tested reduction rates in ternary mixtures according to the following eqs 3 and 4. Reduction errors of permeance and selectivity are obtained from the difference of tested and predicted reductions.

$$\pi_{\text{TP}} = (P_{\text{H}_2} - P'_{\text{H}_2})/P_{\text{H}_2} \times 100\% \quad (1)$$

$$\pi_{\text{T}\alpha} = (\alpha - \alpha')/\alpha \times 100\% \quad (2)$$

$$\pi_{\text{PP}} = [P_{\text{H}_2} - (P_{\text{H}_2} - P_{\text{H}_2} \times \pi_{\text{TP1}}) \times \pi_{\text{TP2}}]/P_{\text{H}_2} \times 100\% \quad (3)$$

$$\pi_{\text{P}\alpha} = [\alpha - (\alpha - \alpha \times \pi_{\text{T}\alpha 1}) \times \pi_{\text{T}\alpha 2}]/\alpha \times 100\% \quad (4)$$

$$\omega_p = (\pi_{\text{PP}} - \pi_{\text{TP}})/\pi_{\text{TP}} \times 100\% \quad (5)$$

$$\omega_\alpha = (\pi_{\text{P}\alpha} - \pi_{\text{T}\alpha})/\pi_{\text{T}\alpha} \times 100\% \quad (6)$$

where π_{TP} is the tested permeance reduction; $\pi_{\text{T}\alpha}$ is the tested selectivity reduction; π_{TP1} , π_{TP2} , $\pi_{\text{T}\alpha 1}$, and $\pi_{\text{T}\alpha 2}$ are the tested permeance and selectivity reductions in two ternary mixtures, respectively; π_{PP} is the predicted permeance reduction in a quaternary mixture; $\pi_{\text{P}\alpha}$ is the predicted selectivity reduction in a quaternary mixture; ω_p is the permeance reduction error; ω_α is the selectivity reduction error; α and α' are the H_2/CH_4 selectivities before and after the addition of one impurity gas; P_{H_2} and P'_{H_2} are the H_2 permeances before and after the addition of one impurity gas.

3. RESULTS AND DISCUSSION

3.1. Adsorption Properties of Si-CHA Zeolite. Figure 1 shows adsorption isotherms for H₂, CH₄, C₂H₆, C₃H₈, and *n*-C₄H₁₀

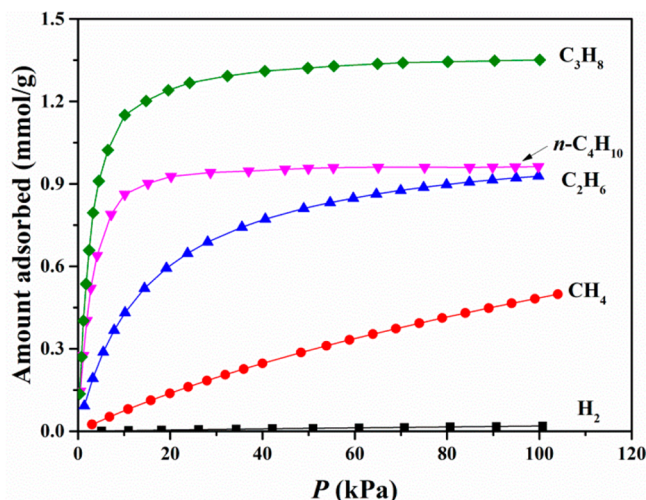


Figure 1. Adsorption isotherms for H₂, CH₄, C₂H₆, C₃H₈, and *n*-C₄H₁₀ on zeolite Si-CHA crystals at 298 K.

C₄H₁₀ on Si-CHA zeolite at 298 K. The absorption amount of CH₄ was several times greater than that of H₂ at the pressure range, indicating that Si-CHA zeolite adsorbs preferentially CH₄ over H₂. The adsorption amount of hydrocarbons at 100 kPa increased with the increase of carbon numbers except for *n*-C₄H₁₀ in the order of CH₄ < C₂H₆ < *n*-C₄H₁₀ < C₃H₈. It could be attributed to the increase of adsorption heat on zeolites.²⁶ The lower loading for *n*-C₄H₁₀ (~0.86 mmol/g) than for C₃H₈ (~1.24 mmol/g) on zeolite Si-CHA might be due to the fact that *n*-C₄H₁₀ is too big (kinetic diameter of 4.3 Å) to diffuse into the zeolite channel (kinetic diameter of 3.8 Å). The adsorption amount for C₃H₈ on SAPO-34 (CHA framework containing P) was ~2.1 mmol/g at 293 K and 80 kPa, which was higher than those for CH₄ and C₂H₆ but lower than that for *n*-C₄H₁₀. The adsorption amount on Si-CHA zeolite for C₃H₈ was 0.45 mmol/g at 78 kPa and 303 K, which was smaller than that for C₂H₆ (2.82 mmol/g).³⁸ The *D* value for C₂H₆ was also ~4 orders of magnitude higher than that for C₃H₈ on zeolite Si-CHA and ITQ-3.³⁸ The differences of absorption properties for hydrocarbons among the literatures could be attributed to the differences of crystal composition and particle sizes.³⁹ The adsorption isotherms of higher hydrocarbons (C₂–C₄) were fit with Langmuir equation, indicating that the crystals were typical microporous materials.³⁸ It is surprising that the adsorption amount of normal butane is lower than that of propane. For a 10-membered-ring MFI zeolite²⁹ with a bigger pore size of 5.5 Å, the adsorption amount increased with the increase of carbon numbers for the linear hydrocarbons from C1 to C5. We

consider that the pore size also influences the loading of hydrocarbons especially for a small-pore zeolite. Si-CHA zeolite has a small pore of 3.8 Å. Normal butane (5.1 Å) is too big to diffuse into the zeolite pores fully. The nanochannels of zeolite cannot be filled fully by the big butane molecules. Therefore, the loading of the normal butane was lower than that of propane.

XRD characterization indicated that the as-synthesized membrane displayed pure CHA phase, as shown in Figure S1. A continuous and intergrown zeolite layer with thickness of 2.5 μm was formed on the surface of tubular porous alumina substrate, as shown in Figure S2.

Concentration polarization became more serious as the pressure increased.⁴⁰ Single-H₂ and -CH₄ permeances dependences of pressure drop and temperature are shown in Figures S3 and S4, respectively. Single-H₂ permeance and ideal H₂/CH₄ selectivity decreased slightly with the increase of temperature. Single-H₂ permeance increased slightly with increase of pressure due to the contribution of defects on H₂ permeance.

3.2. Binary H₂/CH₄ Separation. Separation performances of two Si-CHA zeolite membranes M1 and M2 prepared for 3 and 4 d are listed in Table 1 for an equimolar H₂/CH₄ mixture, respectively. Both membranes displayed high selectivities larger than 80 in the mixture, indicating that they have high quality. Membrane M2 displayed a higher selectivity but a lower H₂ permeance than membrane M1. The mixture selectivity was higher than ideal selectivity for both membranes. It was because H₂ permeation inhibited CH₄ permeation in the mixture separation. The adsorption selectivity of H₂/CH₄ was less than 1 at 100 kPa, as shown in Figure 1, but H₂/CH₄ selectivity was more than 85. Molecular size and the relative adsorption strength determine the faster gas in a binary mixture.⁴¹ Hydrogen has a higher diffusivity but lower coverage in zeolite membrane than CH₄. A high H₂/CH₄ selectivity indicates that separation in the H₂/CH₄ mixture is dominated by diffusion difference/size exclusion between H₂ and CH₄ in the small zeolite channel. Compared with our previous SAPO-34 and SSZ-13 membranes,¹⁷ our current Si-CHA membrane displayed a higher H₂ permeance and higher H₂/CH₄ selectivity.

Figure 2 shows selectivity and permeance through Si-CHA zeolite membrane M1 as a function of pressure drop in an equimolar H₂/CH₄ mixture at 298 K. Si-CHA zeolite membrane M1 displayed a high H₂ permeance of 1.44×10^{-6} mol/(m² s Pa) and H₂/CH₄ selectivity of 85 at 0.2 MPa pressure drop and 298 K for an equimolar H₂/CH₄ mixture. Methane permeance that was mainly accounted to the flow through defects kept constant as pressure increased, indicating that the large defects with viscous flow are seldom and the membrane has high quality.⁴² Hydrogen permeance and H₂/CH₄ selectivity showed similar decline trends. Two factors decreased H₂ permeance along with pressure drop. The coverage of hydrogen molecule on zeolite surface did not

Table 1. Unary and Binary (Equimolar H₂/CH₄) Gas Permeation Properties of the Typical Si-CHA Zeolite Membranes M1 and M2 at 298 K, 0.2 MPa Pressure Drop, and 4.0 SLPM Total Feed Flow Rate

number	single-gas permeance [mol/(m ² s Pa)]		ideal selectivity	permeance in mixture [mol/(m ² s Pa)]		separation selectivity
	H ₂ × 10 ⁻⁷	CH ₄ × 10 ⁻⁹		H ₂ × 10 ⁻⁷	CH ₄ × 10 ⁻⁹	
M1	14.6	20.3	71.6	14.4	16.9	85.0
M2	4.8	6.5	74.4	5.5	5.1	106

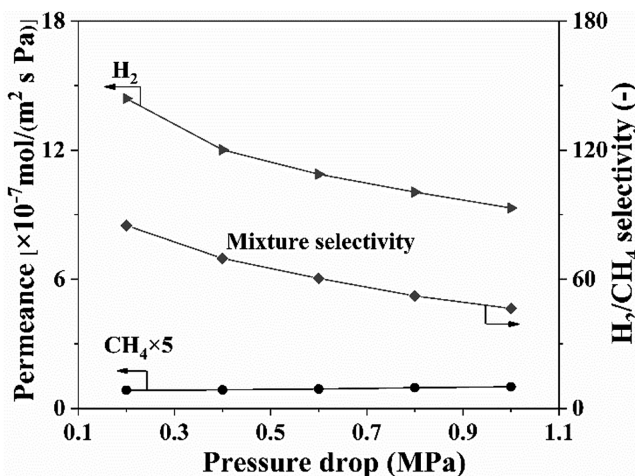


Figure 2. Pressure dependence of H_2 and CH_4 permeances and H_2/CH_4 selectivity of Si-CHA zeolite membrane M1 for an equimolar H_2/CH_4 mixture at 298 K and 4.0 SLPM feed flow rate.

increase linearly with pressure, and therefore, the increase rate of H_2 flux was slower than that of pressure drop. The other factor was concentration polarization, which damaged the permeance and selectivity especially for a high permeable and selective membrane.⁴³ Concentration polarization became more serious as pressure increased.⁴⁰

Figure 3 illuminates selectivity and permeance through Si-CHA zeolite membrane M1 as a function of temperature for an

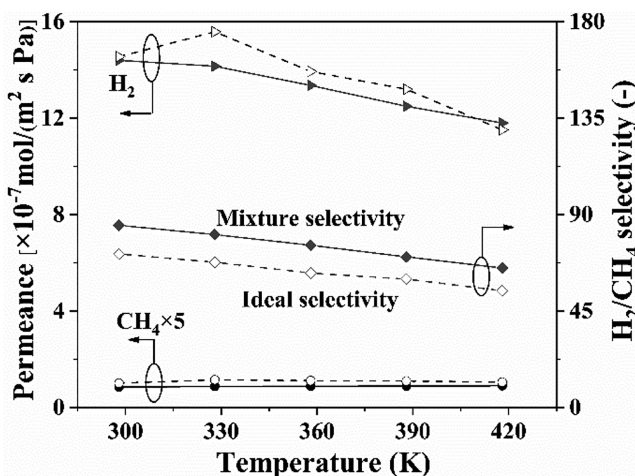


Figure 3. Temperature dependence of H_2 and CH_4 permeances and H_2/CH_4 selectivity of Si-CHA zeolite membrane M1 for an equimolar H_2/CH_4 mixture at 0.2 MPa pressure drop and 4.0 SLPM feed flow rate.

equimolar H_2/CH_4 mixture at 0.2 MPa pressure drop. Single-gas permeances for H_2 and CH_4 were included. Mixture CH_4 permeance was lower than single- CH_4 permeance in the temperature range at 0.2 MPa. It suggests that some H_2 molecules permeate through defect pores and inhibit the permeation of CH_4 . Hydrogen permeance in the mixture was much closer to single- H_2 permeance, indicating that the permeation of CH_4 hardly influences that of H_2 because most of CH_4 permeated through defects and the defect concentration was very low. Hydrogen permeance decreased with temperature. The adsorption of H_2 on the surface of zeolite membrane became weaker when temperature increased. On

the contrary, the diffusion rate of hydrogen through the membrane increased with temperature. The permeance of gas through a zeolite membrane was the competition result of preferential adsorption and competitive diffusion.⁴¹ Therefore, gas permeance decreased with temperature (starting from low temperatures) until the permeation was primarily dominated by competitive diffusion at higher temperatures. It caused a minimum in permeance in a large temperature range. The minimum of H_2 permeance was not observed in this current study because the test at a higher temperature was not carried out by the temperature limit of rubber O-rings. A similar decrease trend of hydrogen permeance along with temperature was found in H_2/CH_4 separation using our previous SSZ-13 membranes.¹⁷

Hydrogen permeance and H_2/CH_4 selectivity increased with feed H_2 concentration, as shown in Figure 4. Hydrogen

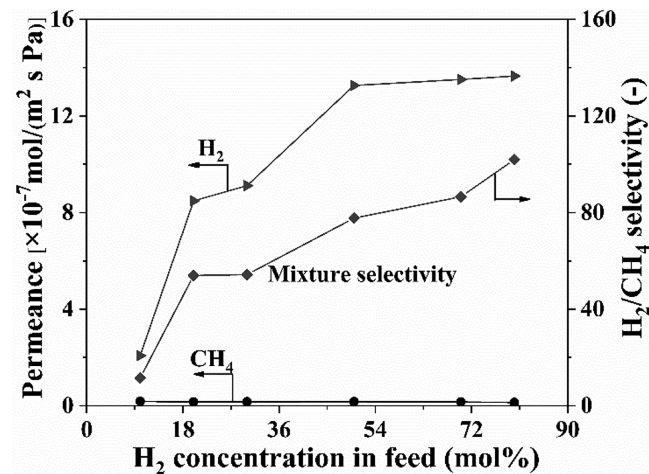


Figure 4. Feed H_2 concentration dependence of N_2 and CH_4 permeances and H_2/CH_4 selectivity of Si-CHA zeolite membrane M1 at 298 K, 0.2 MPa pressure drop, and 4.0 SLPM feed flow rate.

permeance first increased fast and then slowly increased when the feed H_2 concentration increased from 10 to 50 mol % and then to 80 mol %, respectively. Methane permeance decreased slightly as the feed H_2 concentration increased. Hydrogen permeance increased by a factor of 5 when the feed H_2 concentration increased from 10 to 50 mol %. Similar trends were found in H_2/CH_4 separation using SAPO-34 and SSZ-13 membranes.¹⁷ The coverage of methane on the surface of zeolite decreased when the bulk hydrogen concentration increased. Once a trace of methane diffused into zeolite pores when the bulk concentration of preferentially adsorbed methane was high, the diffusion of hydrogen was inhibited by methane diffusion to a large extent. Therefore, H_2 permeance increased greatly when its concentration in feed increased from 10 to 50 mol %. It was different from that in CO_2/CH_4 separation.¹⁷ The permeance of preferentially adsorbed CO_2 changed a little when CO_2 concentration increased from 10 to 50 mol %.

3.3. Ternary Separation. **3.3.1. $H_2/CH_4/C_2H_6$ Separation.** Figure 5 reveals the time course of permeances and H_2/CH_4 selectivity of Si-CHA zeolite membrane M1 for the separation of ternary $H_2/CH_4/C_2H_6$ mixtures. Ethane is the common impurity gas in H_2/CH_4 mixtures from ethylene industry and purge gas. Hydrogen permeance decreased by 54.2% and 62.6%, but methane permeance decreased a little when 1 and 5 mol % ethane was added, respectively. Thus, H_2/CH_4

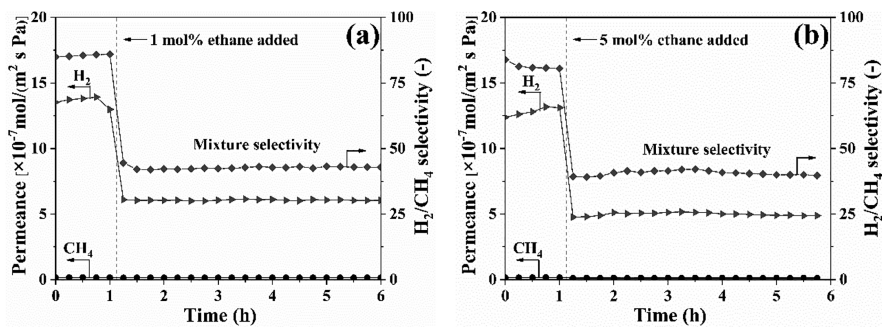


Figure 5. Time course of permeances and H_2/CH_4 selectivity of Si-CHA zeolite membrane M1 for an equimolar H_2/CH_4 mixture containing (a) 1 and (b) 5 mol % ethane at 298 K, 0.2 MPa pressure drop, and 4.0 SLPM feed flow rate.

selectivity declined by 49.8% and 50.6% (also shown in Table 2). It took only 0.5 h to reach the stable separation

Table 2. Reduction in H_2 Permeance and H_2/CH_4 Selectivity for Ternary Mixture Separations Containing Impurity Gases at 298 K

impurities (partial pressure)	π_{TP} (%)	π_o (%)
1 mol % C_2H_6 (2 kPa)	54.2	49.8
5 mol % C_2H_6 (10 kPa)	62.6	50.6
1 mol % C_3H_8 (2 kPa)	54.2	18.5
5 mol % C_3H_8 (10 kPa)	69.3	30.1
5 mol % $n-C_4H_{10}$ (10 kPa)	65.3	21.2
1.6 mol % H_2O (3.2 kPa)	63.0	29.8

performance. Wu et al.³³ reported that CO_2 permeance and CO_2/CH_4 selectivity of a SAPO-34 membrane decreased by 35% and 6%, respectively, when 5 mol % ethane was added to the feed. The adsorption amount of CO_2 is much greater than those of methane and ethane. Therefore, the loading of ethane on SAPO-34 pores did not significantly weaken the adsorption site and the diffusivity of the fast-permeating species of CO_2 in SAPO-34 pores. In our current H_2/CH_4 mixture, the loading of ethane in Si-CHA zeolite pores should decrease the H_2 loading more than CH_4 in zeolite pores because the adsorption capacity of ethane is greater than that of methane and much greater than that of hydrogen (Figure 1). Meanwhile, the loading of ethane inhibited the diffusion of H_2 through the zeolite pore but influenced the diffusion of methane less since most of methane went through the defects. A permeance is a product of loading and diffusivity. Thus, the decrease percentages of H_2 permeance and H_2/CH_4 selectivity were over 50%, which were higher than that in the CO_2/CH_4

mixture through SAPO-34 membrane³³ when 5 mol % ethane was added. The same type of membrane (SSZ-13) with less Si/Al ratio in the framework showed little change in separation performance in the CO_2/CH_4 system with the addition of ethane.³³ Similar trends of permeance and selectivity of membrane M2 were found when 5 mol % ethane was added, as shown in Figure S5.

Increasing the feed pressure improved the partial pressure of ethane, and therefore, H_2 permeance and H_2/CH_4 selectivity decreased with a similar rate by the inhabitation of ethane diffusion in the ternary $H_2/CH_4/C_2H_6$ mixture (Figure 6a). Methane diffused most through the defects, and its permeance was almost independent of pressure and temperature (Figure 6). Increasing temperature in a certain range can benefit the coverage and diffusivity of H_2 by means of reducing the coverage of preferentially adsorbed ethane. At a higher temperature, the coverage of H_2 decreased, resulting probably in the decrease of H_2 permeance. Therefore, H_2 permeance had a maximum as shown Figure 6b. It is different from the relation of temperature with H_2 permeance in a binary mixture (Figure 3). But, it is similar to the trend of H_2 permeance as a function of temperature for ternary $H_2/CH_4/H_2O$ mixture through CHA zeolite membranes in our previous report.¹⁷

A trace of ethane was detected in the permeated gas. Ethane permeance was as low as $(3\text{--}9) \times 10^{-10} \text{ mol}/(\text{m}^2 \cdot \text{s Pa})$ during the tested ranges of pressure drop and temperature, as shown in Figure S6. Ethane permeance decreased with the increase of pressure drop and temperature. The H_2/C_2H_6 selectivities were as high as 350–1400 with an ethane concentration of 0.7–2.8 mol%.

3.3.2. $H_2/CH_4/C_3H_8$ Separation. Hydrogen permeance decreased by 54.2% and 69.3%, and H_2/CH_4 selectivity declined by 18.5% and 30.1% when 1 and 5 mol % propane

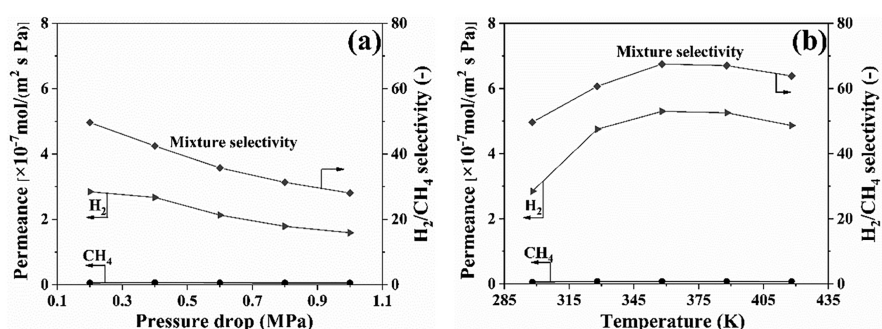


Figure 6. Permeances and H_2/CH_4 selectivity of Si-CHA zeolite membrane M2 as functions of (a) pressure drop and (b) temperature for a $H_2/CH_4/C_2H_6$ (47.5/47.5/5) ternary mixture at a 1.0 SLPM feed flow rate.

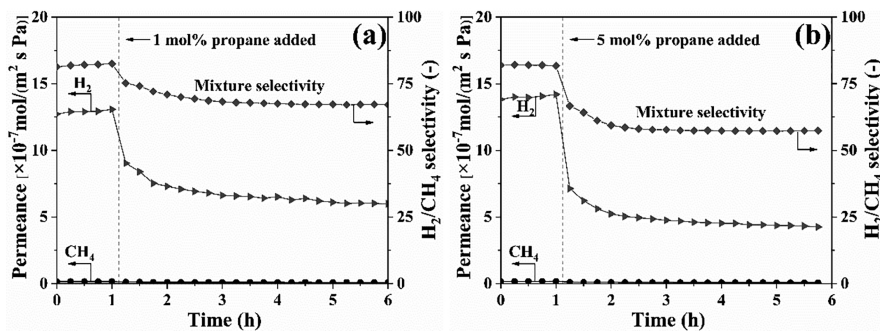


Figure 7. Time course of permeances and H_2/CH_4 selectivity of Si-CHA zeolite membrane M1 for an equimolar H_2/CH_4 mixture containing (a) 1 mol % propane added and (b) 5 mol % propane added at 298 K, 0.2 MPa pressure drop, and 4.0 SLPM feed flow rate.

was added into the feed, respectively, as shown in Figure 7 and Table 2. The declined percentages were much closer to these when the same amount of ethane was added, as shown in Figure 5. Hydrogen permeance reached an almost steady state after 6 h and a complete steady state after 12 h. Separation selectivity was stable after only 2 h. Similar trends for permeance and selectivity of the membrane M2 were detected when 5 mol % propane was added, as shown in Figure S7. In the separation systems containing two compositions of weakly adsorbed on zeolites such as N_2/CH_4 ³³ and H_2/N_2 ²⁶ mixtures, the steady state for the fast-permeating gas cannot be achieved through SSZ-13 or SAPO-34 membranes even after several days. The authors considered that propane (4.1 Å) molecules in the hydrophilic SAPO-34 and Al-containing SSZ-13 permeated very slowly through 8-member-ring pores (3.8 Å), and therefore, permeance of fast-permeating gas reduced greatly and hardly reached the steady state. Nitrogen permeance of SSZ-13 membrane decreased by 44% after 7 d in N_2/CH_4 mixture, and H_2 permeance of SAPO-34 membrane declined by nearly 50% in the H_2/N_2 mixture. Propane with the concentration of 0.098 mol % was found in the permeated gas mixtures.^{26,33} The steady state was observed after adding 5 mol % propane in our system using Si-CHA zeolite membranes that were more hydrophobic than SSZ-13 and SAPO-34 membranes. The weak adsorption of propane on the hydrophobic Si-CHA zeolite resulted in a lower loading amount (shown in Figure 1) than those on SSZ-13 and SAPO-34.^{26,30,33} Thus, propane had less probabilities to enter the pores and was easier to pass for Si-CHA membrane than the other two. Propane concentration in the permeated gas was out of the detection limit in our system. It also supported the above conclusion. In the mixture with a polar adsorbate over a nonpolar one such as CO_2/CH_4 , the separation performance of SSZ-13 membrane reached the steady state but that of SAPO-34 membrane did not when 5 mol % propane was added.^{30,33}

Note that H_2 permeance and H_2/CH_4 selectivity decreased only 1%–15% more when the addition of ethane and propane increased by a factor of 4 from 1 to 5 mol % (as shown in Figures 5 and 7). It indicates that the decrease in separation performance of Si-CHA zeolite membranes is not in proportion to partial pressure (concentration) of the third gas.

3.3.3. $H_2/CH_4/n-C_4H_{10}$ Separation. Figure 8 shows the time course of permeances and H_2/CH_4 selectivity of Si-CHA zeolite membrane M2 for an H_2/CH_4 mixture containing 5 mol % *n*-butane. The influence of *n*-butane on the separation performance of Si-CHA zeolite membrane M2 was equivalent to those of propane and ethane. The stable separation

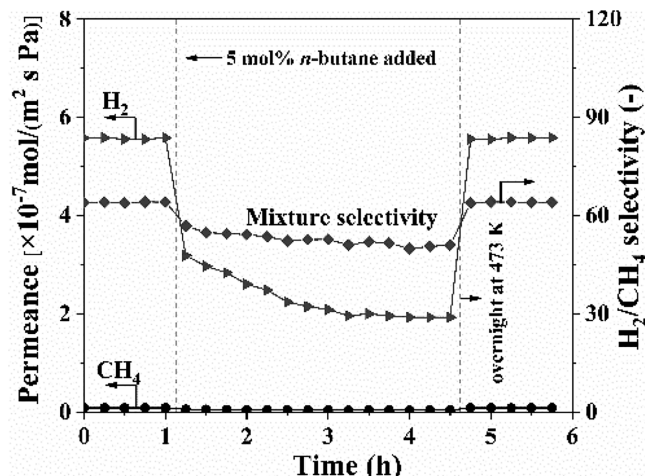


Figure 8. Time course of permeances and H_2/CH_4 selectivity of Si-CHA zeolite membrane M2 for a $H_2/CH_4/n-C_4H_{10}$ (47.5/47.5/5) ternary mixture at 298 K, 0.1 MPa pressure drop, and 4.0 SLPM feed flow rate.

performance was achieved after 4 h. Hydrogen permeance and H_2/CH_4 selectivity declined by 65.3% and 21.2% when 5 mol % *n*-butane was included, respectively. The concentration of *n*-butane in the permeate side was also beyond the detection limit of GC, similar to the result with the addition of propane. It also confirmed the high quality of the Si-CHA zeolite membrane. Li et al.³⁰ reported that CO_2 permeance and CO_2/CH_4 selectivity declined by 59% and 42% when only 1 mol % *n*-butane was added. Carbon dioxide is a polar adsorbate to reduce the loading of higher hydrocarbons compared with hydrogen, as shown in Figure 1. However, the SAPO-34 membrane was more sensitive to the impurity of *n*-butane in CO_2/CH_4 separation than our Si-CHA zeolite membrane in H_2/CH_4 separation. It further indicates that hydrophobic zeolite membranes are influenced less than the hydrophilic zeolite membranes by the impurities of higher hydrocarbons.

Table 2 summarizes the effects of single impurity on the separation performance of Si-CHA zeolite membrane for H_2/CH_4 separations. The influence of the impurity on H_2 permeance decreased in the order of $H_2O > C_3H_8 > C_4H_{10} > C_2H_6$. Water had the highest loading in CHA zeolite.³⁰ Therefore, this order agreed with the adsorption amount of these impurity gas, as shown in Figure 1. It indicated that increasing the temperature at a certain range was an effective way to reduce the influence of the impurity gas on separation performance, as shown in Figure 6b.

3.4. Quaternary $\text{H}_2/\text{CH}_4/\text{C}_2\text{H}_6/\text{C}_3\text{H}_8$ and $\text{H}_2/\text{CH}_4/\text{H}_2\text{O}/\text{C}_3\text{H}_8$ Separations. The literatures always report the effect of single impurity on the separation performance of zeolite membranes in the ternary mixtures.^{26,27,30,33,44,45} The influence of two impurity gases on the separation performance of Si-CHA zeolite membrane was investigated for the quaternary mixtures in this section. The time course of permeances and H_2/CH_4 selectivity of Si-CHA zeolite membrane M2 for a quaternary $\text{H}_2/\text{CH}_4/\text{C}_3\text{H}_8/\text{C}_2\text{H}_6$ (45/45/5/5) mixture is shown in Figure 9. The total tested reductions of H_2

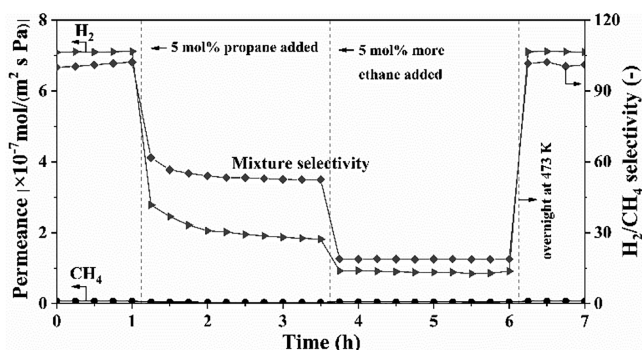


Figure 9. Time course of permeances and H_2/CH_4 selectivity of Si-CHA zeolite membrane M2 for a ternary $\text{H}_2/\text{CH}_4/\text{C}_3\text{H}_8$ (47.5/47.5/5) mixture and a quaternary $\text{H}_2/\text{CH}_4/\text{C}_3\text{H}_8/\text{C}_2\text{H}_6$ (45/45/5/5) mixture at 298 K, 0.2 MPa pressure drop, and 4.0 SLPM feed flow rate.

permeance (π_{TP}) and H_2/CH_4 selectivity (π_{Ta}) through Si-CHA zeolite membrane M2 were 87.3% and 81.6% when 5 mol % propane and 5 mol % ethane were added to the feed, respectively, as shown in Figure 9 and Table 3. It can be seen from Table 3 that the predicted H_2 permeance reduction (π_{PP}) and H_2/CH_4 selectivity reduction (π_{Pa}) are 88.5% and 65.5%, respectively. As shown in eqs 3 and 4, the predicted influence of two impurities is the simple overlap of the influence of each one shown in Table 2. The error of predicted H_2 permeance over tested one was as low as 1.38%. The error of predicted and tested H_2/CH_4 selectivity was a little bit high (-24.6%). It was because the permeation of CH_4 through the defects did not obey the separation mechanism of surface diffusion. Methane permeance decreased little when the second impurity gas was added, which was different to that by prediction from Table 2. As a consequence, the tested selectivity was lower than the predicted one. A similar phenomenon was found in a quaternary $\text{H}_2/\text{CH}_4/\text{H}_2\text{O}/\text{C}_3\text{H}_8$ (46.7/46.7/1.6/5) mixture, as shown in Figure 10 and Table 3. The error of predicted H_2 permeance over the tested one was only 9.97%. The low errors in the two mixtures showed that the prediction fit with H_2 permeance through our Si-CHA zeolite membranes when multi impurities were contained. Please note that the membrane was a different batch for the tests in ternary and quaternary mixtures in Tables 2 and 3, respectively.

Table 3. Tested and Predicted Reductions and Error in H_2 Permeance and H_2/CH_4 Selectivity for Quaternary Mixture Separations Containing Impurity Gases at 298 K^a

quaternary system	π_{TP} (%)	π_{Ta} (%)	π_{PP} (%)	π_{Pa} (%)	ω_P (%)	ω_a (%)
$\text{H}_2/\text{CH}_4/\text{C}_3\text{H}_8/\text{C}_2\text{H}_6$	87.3	81.6	88.5	65.5	+1.38	-24.6
$\text{H}_2/\text{CH}_4/\text{H}_2\text{O}/\text{C}_3\text{H}_8$	79.8	64.2	88.6	50.9	+9.97	-26.1

^aNote: prediction from the results for ternary mixtures from Table 2.

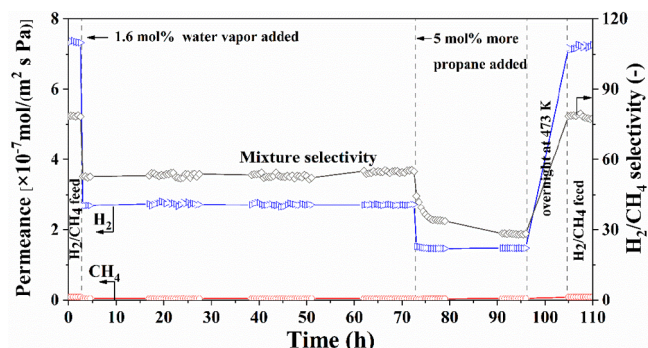


Figure 10. Time course of permeances and H_2/CH_4 selectivity of Si-CHA zeolite membrane M3 for a ternary $\text{H}_2/\text{CH}_4/\text{H}_2\text{O}$ (48.2/48.2/1.6) mixture and a quaternary $\text{H}_2/\text{CH}_4/\text{H}_2\text{O}/\text{C}_3\text{H}_8$ (46.7/46.7/1.6/5) mixture at 298 K, 0.2 MPa pressure drop, and 1.0 SLPM feed flow rate.

In the quaternary $\text{H}_2/\text{CH}_4/\text{H}_2\text{O}/\text{C}_3\text{H}_8$ mixture, the relative humidity in this mixture was almost 100% at 298 K. This humidity was higher than that in actual situations. The loading of water vapor is the highest among all the investigated impurity gases on zeolite.³⁰ The permeance of the low-silica CHA zeolite membrane was close to zero because water vapor was easily adsorbed on hydrophilic zeolites and blocked their pores^{16,27} at low temperatures. Herein, we found that the pores of Si-CHA zeolite membranes were still open for gas transports with good selectivity. It was because the current membrane displayed good resistance to water vapor due to its hydrophobic property of the all-silica framework. Separation performance of the current membrane was stable during the continuous test for over 70 h. It took at least 7 h to reach the steady state when 5 mol % propane was added in this quaternary mixture. But, it took only 2 h to reach steady state in the ternary mixture when 5 mol % propane was added (Figure 7). We consider that the existence of water vapor as the other impurity gas could be responsible for the longer time before stabilization in the quaternary mixture. The competitive adsorption in the quaternary mixture (Figure 10) is more complicated than that in the ternary mixture (Figure 7), which might result in a longer time to reach steady state during the separation process of membrane. Please note that 7 h was a short time to reach steady state compared with those in the literatures.^{26,33}

3.5. Comparison to the Literatures. Figure 11a shows the comparison of separation performance of our Si-CHA zeolite membrane M1 with those of polymeric and inorganic membranes in Robeson plot in 2008.⁴³ Permeability was permeance multiplied by membrane thickness. Only single-gas permeance and ideal H_2/CH_4 selectivity were reported for SSZ-13,¹⁵ SAPO-17,⁴⁶ and SAPO-34¹⁷ membranes. The data of separation performance and thickness of zeolite and MOF membranes in the literatures are also listed in Table S1. Compared with the polymeric membranes, inorganic mem-

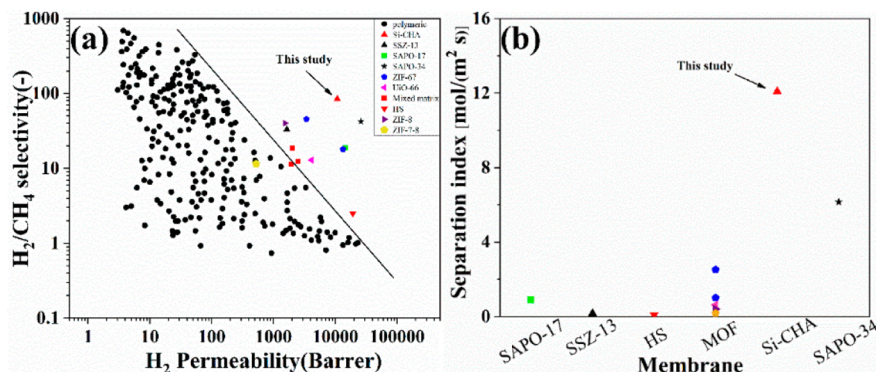


Figure 11. Comparison of the separation performance of our Si-CHA (symbol red ▲) membrane with polymeric membranes with symbol black ● present (a) in the H_2/CH_4 separation Robeson plot and (b) separation index plot with other membranes: ZIF-67^{48,49} with symbol purple ♦, ZIF-7-8⁵⁰ with symbol gold ♠, SAPO-34¹⁷ with symbol black ★, SSZ-13¹⁵ with symbol black ▲, ZIF-8⁴⁷ with symbol purple ▽, UIO-66²⁴ with symbol pink ◀, SAPO-17⁴⁶ with symbol green ■, and HS²¹ with symbol red ▼ membranes and mixed-matrix membranes^{51–53} with symbol red ■.

branes^{15,46,47} had better H_2/CH_4 separation performances. Zhou et al.¹⁷ synthesized a SAPO-34 membrane with H_2 permeance of 1.45×10^{-6} mol/(m² s Pa) (H_2 permeability of 25980 barrers) and H_2/CH_4 selectivity of 42.2 at 298 K and 200 kPa pressure drop. Zhong et al.⁴⁷ prepared a 12 μ m thick SAPO-17 membrane; the membrane displayed a single-gas H_2 permeance of 4.0×10^{-7} mol/(m² s Pa) (H_2 permeability of 14400 barrers) and ideal H_2/CH_4 selectivity of 19.0 at 298 K and 303 kPa. Herein, the Si-CHA zeolite membrane M1 with a thickness of 2.5 μ m displayed H_2 permeance of 1.44×10^{-6} mol/(m² s Pa) (H_2 permeability of 10800 barrers) and H_2/CH_4 selectivity of 85.0. Figure 11b shows the comparison of our membrane M1 with other zeolite and MOF membranes in a separation index plot. Our membrane displayed a separation index of 12.10 mol/(m² s) for H_2/CH_4 separation, which was twice or higher than those of other reported membranes, as shown in Figure 11b. It shows that our current membrane displayed the highest separation performance among the reported membranes. Compared with the previous SSZ-13 membranes,¹⁵ the current Si-CHA zeolite membrane had few cations in the zeolite nanochannels. Therefore, the transfer resistance of the current membrane was considered to be lower than that of our previous SSZ-13 membrane.¹⁵ Moreover, the thinner membrane of the current Si-CHA zeolite membrane could be responsible for the higher H_2 permeance.

4. CONCLUSIONS

The best Si-CHA zeolite membrane had a H_2/CH_4 selectivity of 85.0 and a H_2 permeance of 1.44×10^{-6} mol/(m² s Pa) (permeability of 10800 barrers) for an equimolar H_2/CH_4 mixture at 0.2 MPa pressure drop and 298 K. The membrane displayed the best integrated separation performance among the current polymeric and inorganic membranes. Hydrogen permeance and H_2/CH_4 selectivity of Si-CHA zeolite membrane decreased with the increase of temperature and pressure for binary H_2/CH_4 separations. A third gas (C_2H_6 , C_3H_8 , *n*-butane, and water vapor) decreased the H_2 permeance of the membrane in the order similar to the adsorption amount in Si-CHA zeolite. When two impurity gases were added, the tested reduction percentages in H_2 permeance and H_2/CH_4 selectivity were close to the predicted ones by simply overlapping the reduction of each impurity. Separation performance of the membranes in all the tests with impurity

gases reached a stable value within several hours. Increasing the temperature decreased the reduction of separation performance of the membrane by the tested impurity gases. Separation performance of the membrane could be recovered when the impurity gases were removed. The membrane had good stability in the wet mixture. Our results show that Si-CHA zeolite membranes have potential for actual application of H_2/CH_4 mixtures containing impurities.

■ ASSOCIATED CONTENT

Supporting Information

The Supporting Information is available free of charge at <https://pubs.acs.org/doi/10.1021/acs.energyfuels.0c01720>.

Discussion of experimental processes used, figures of SEM images, XRD patterns, pressure and temperature dependence of single-gas permeances, time course of permeances and H_2/CH_4 selectivity, and H_2/C_2H_6 selectivity as a function of pressure drop and temperature, and table of summary of test conditions (PDF)

■ AUTHOR INFORMATION

Corresponding Authors

Shenglai Zhong – State Key Laboratory of Materials-Oriented Chemical Engineering, College of Chemical Engineering, Nanjing Tech University, Nanjing 210009, P. R. China;
Email: zhong@njtech.edu.cn

Rongfei Zhou – State Key Laboratory of Materials-Oriented Chemical Engineering, College of Chemical Engineering, Nanjing Tech University, Nanjing 210009, P. R. China;
ORCID: [0000-0003-0305-252X](https://orcid.org/0000-0003-0305-252X); Phone: +86-25-6880-3018; Email: rf-zhou@njtech.edu.cn; Fax: +86-25-8317-2261

Authors

Tangyin Wu – State Key Laboratory of Materials-Oriented Chemical Engineering, College of Chemical Engineering, Nanjing Tech University, Nanjing 210009, P. R. China

Chaojiu Shu – State Key Laboratory of Materials-Oriented Chemical Engineering, College of Chemical Engineering, Nanjing Tech University, Nanjing 210009, P. R. China

Shuai Liu – State Key Laboratory of Materials-Oriented Chemical Engineering, College of Chemical Engineering, Nanjing Tech University, Nanjing 210009, P. R. China

Boshen Xu – State Key Laboratory of Materials-Oriented Chemical Engineering, College of Chemical Engineering, Nanjing Tech University, Nanjing 210009, P. R. China

Complete contact information is available at:
<https://pubs.acs.org/10.1021/acs.energyfuels.0c01720>

Notes

The authors declare no competing financial interest.

ACKNOWLEDGMENTS

We gratefully acknowledge the financial support of this study from National Key Research and Development Program of China (2017YFB0603402) and the National Natural Science Foundations of China (21576131, 21938007, and 21921006).

REFERENCES

- (1) Müller, K.; Thiele, S.; Wasserscheid, P. Evaluations of concepts for the integration of fuel cells in liquid organic hydrogen carrier systems. *Energy Fuels* **2019**, *33* (10), 10324–10330.
- (2) Kolb, G.; Keller, S.; O'Connell, M.; Pecov, S.; Schuerer, J.; Spasova, B.; Tiemann, D.; Ziogas, A. Microchannel fuel processors as a hydrogen source for fuel cells in distributed energy supply systems. *Energy Fuels* **2013**, *27* (8), 4395–4402.
- (3) Salaudeen, S. A.; Acharya, B.; Heidari, M.; Al-Salem, S. M.; Dutta, A. Hydrogen-rich gas stream from steam gasification of biomass: eggshell as a CO₂ sorbent. *Energy Fuels* **2020**, *34* (4), 4828–4836.
- (4) Nenoff, T.; Spontak, R.; Aberg, C. Membranes for hydrogen purification: an important step toward a hydrogen-based economy. *MRS Bull.* **2006**, *31* (10), 735–741.
- (5) Bernardo, G.; Araujo, T.; da Silva Lopes, T.; Sousa, J.; Mendes, A. Recent advances in membrane technologies for hydrogen purification. *Int. J. Hydrogen Energy* **2020**, *45* (12), 7313–7338.
- (6) Grande, C. A. *PSA technology for H₂ separation*; Wiley-VCH Verlag, 2016; Vol. 1, pp 491–508.
- (7) Jiang, X.; Li, S.; Shao, L. Pushing CO₂-philic membrane performance to the limit by designing semi-interpenetrating networks (SIPN) for sustainable CO₂ separations. *Energy Environ. Sci.* **2017**, *10* (6), 1339–1344.
- (8) Zhang, Y.; Cheng, X.; Jiang, X.; Urban, J. J.; Lau, C. H.; Liu, S.; Shao, L. Robust natural nanocomposites realizing unprecedented ultrafast precise molecular separations. *Mater. Today* **2020**, *36*, 40.
- (9) Jiang, X.; Li, S.; Bai, Y.; Shao, L. Ultra-facile aqueous synthesis of nanoporous zeolitic imidazolate framework membranes for hydrogen purification and olefin/paraffin separation. *J. Mater. Chem. A* **2019**, *7* (18), 10898–10904.
- (10) Huang, A.; Liu, Q.; Wang, N.; Zhu, Y.; Caro, J. Bicontinuous zeolitic imidazolate framework ZIF-8@GO membrane with enhanced hydrogen selectivity. *J. Am. Chem. Soc.* **2014**, *136* (42), 14686–14689.
- (11) Sun, Y.; Liu, Y.; Caro, J.; Guo, X.; Song, C.; Liu, Y. In-plane epitaxial growth of highly c-oriented NH₂-MIL-125(Ti) membranes with superior H₂/CO₂ selectivity. *Angew. Chem., Int. Ed.* **2018**, *57* (49), 16088–16093.
- (12) Kanezashi, M.; O'Brien-Abraham, J.; Lin, Y. S.; Suzuki, K. Gas permeation through DDR-type zeolite membranes at high temperatures. *AIChE J.* **2008**, *54* (6), 1478–1486.
- (13) Zhu, M.; Liang, L.; Wang, H.; Liu, Y.; Wu, T.; Zhang, F.; Li, Y.; Kumakiri, I.; Chen, X.; Kita, H. Influences of acid post-treatment on high silica SSZ-13 zeolite membrane. *Ind. Eng. Chem. Res.* **2019**, *58* (31), 14037–14043.
- (14) Jang, E.; Hong, S.; Kim, E.; Choi, N.; Cho, S. J.; Choi, J. Organic template-free synthesis of high-quality CHA type zeolite membranes for carbon dioxide separation. *J. Membr. Sci.* **2018**, *549*, 46–59.
- (15) Liu, B.; Zhou, R.; Bu, N.; Wang, Q.; Zhong, S.; Wang, B.; Hidetoshi, K. Room-temperature ionic liquids modified zeolite SSZ-13 membranes for CO₂/CH₄ separation. *J. Membr. Sci.* **2017**, *524*, 12–19.
- (16) Liu, B.; Zhou, R.; Yogo, K.; Kita, H. Preparation of CHA zeolite (chabazite) crystals and membranes without organic structural directing agents for CO₂ separation. *J. Membr. Sci.* **2019**, *573*, 333–343.
- (17) Song, S.; Gao, F.; Zhang, Y.; Li, X.; Zhou, M.; Wang, B.; Zhou, R. Preparation of SSZ-13 membranes with enhanced fluxes using asymmetric alumina supports for N₂/CH₄ and CO₂/CH₄ separations. *Sep. Purif. Technol.* **2019**, *209*, 946–954.
- (18) Tang, H.; Bai, L.; Wang, M.; Zhang, Y.; Li, M.; Wang, M.; Kong, L.; Xu, N.; Zhang, Y.; Rao, P. Fast synthesis of thin high silica SSZ-13 zeolite membrane using oil-bath heating. *Int. J. Hydrogen Energy* **2019**, *44* (41), 23107–23119.
- (19) Yu, L.; Nobandegani, M. S.; Holmgren, A.; Hedlund, J. Highly permeable and selective tubular zeolite CHA membranes. *J. Membr. Sci.* **2019**, *588*, 117224.
- (20) Mei, W.; Du, Y.; Wu, T.; Gao, F.; Wang, B.; Duan, J.; Zhou, J.; Zhou, R. High-flux CHA zeolite membranes for H₂ separations. *J. Membr. Sci.* **2018**, *565*, 358–369.
- (21) Fasolin, S.; Romano, M.; Boldrini, S.; Ferrario, A.; Fabrizio, M.; Armelao, L.; Barison, S. Single-step process to produce alumina supported hydroxy-sodalite zeolite membranes. *J. Mater. Sci.* **2019**, *54* (3), 2049–2058.
- (22) Luo, S.; Zhang, Q.; Zhu, L.; Lin, H.; Kazanowska, B.; Doherty, C.; Hill, A.; Gao, P.; Guo, R. Highly selective and permeable microporous polymer membranes for hydrogen purification and CO₂ removal from natural gas. *Chem. Mater.* **2018**, *30* (15), 5322–5332.
- (23) Nian, P.; Li, Y.; Zhang, X.; Cao, Y.; Liu, H.; Zhang, X. ZnO nanorod-induced heteroepitaxial growth of SOD type Co-Based zeolitic imidazolate framework membranes for H₂ separation. *ACS Appl. Mater. Interfaces* **2018**, *10* (4), 4151–4160.
- (24) Friebe, S.; Geppert, B.; Steinbach, F.; Caro, J. Metal-organic framework UIO-66 layer: A highly oriented membrane with good selectivity and hydrogen permeance. *ACS Appl. Mater. Interfaces* **2017**, *9* (14), 12878–12885.
- (25) Ma, X.; Li, Y.; Huang, A. Synthesis of nano-sheets seeds for secondary growth of highly hydrogen permselective ZIF-95 membranes. *J. Membr. Sci.* **2020**, *597*, 117629.
- (26) Chisholm, N. O.; Anderson, G. C.; McNally, J. F.; Funke, H. H.; Noble, R. D.; Falconer, J. L. Increasing H₂/N₂ separation selectivity in CHA zeolite membranes by adding a third gas. *J. Membr. Sci.* **2015**, *496*, 118–124.
- (27) Hong, S.; Kim, D.; Jeong, Y.; Kim, E.; Jung, J. C.; Choi, N.; Nam, J.; Yip, A. C. K.; Choi, J. Healing of microdefects in SSZ-13 membranes via filling with dye molecules and its effect on dry and wet CO₂ separations. *Chem. Mater.* **2018**, *30* (10), 3346–3358.
- (28) Huang, L.; Wang, H.; Chen, J.; Wang, Z.; Sun, J.; Zhao, D.; Yan, Y. Synthesis, morphology control, and properties of porous metal-organic coordination polymers. *Microporous Mesoporous Mater.* **2003**, *58* (2), 105–114.
- (29) Lee, J. B.; Funke, H. H.; Noble, R. D.; Falconer, J. L. High selectivities in defective MFI membranes. *J. Membr. Sci.* **2008**, *321* (2), 309–315.
- (30) Li, S.; Alvarado, G.; Noble, R. D.; Falconer, J. L. Effects of impurities on CO₂/CH₄ separations through SAPO-34 membranes. *J. Membr. Sci.* **2005**, *251* (1), 59–66.
- (31) Li, Y.; Yang, R. T. Gas adsorption and storage in metal-organic framework MOF-177. *Langmuir* **2007**, *23* (26), 12937–12944.
- (32) Tan, K.; Nijem, N.; Gao, Y.; Zuluaga, S.; Li, J.; Thonhauser, T.; Chabal, Y. J. Water interactions in metal organic frameworks. *CrystEngComm* **2015**, *17* (2), 247–260.
- (33) Wu, T.; Diaz, M. C.; Zheng, Y.; Zhou, R.; Funke, H. H.; Falconer, J. L.; Noble, R. D. Influence of propane on CO₂/CH₄ and N₂/CH₄ separations in CHA zeolite membranes. *J. Membr. Sci.* **2015**, *473*, 201–209.
- (34) Zhou, J.; Gao, F.; Sun, K.; Jin, X.; Zhang, Y.; Liu, B.; Zhou, R. Green synthesis of highly CO₂-selective CHA zeolite membranes in

- all-silica and fluoride-free solution for CO₂/CH₄ separations. *Energy Fuels*, just accepted, 2020.
- (35) Kim, E.; Cai, W.; Baik, H.; Choi, J. Uniform Si-CHA zeolite layers formed by a selective sonication-assisted deposition method. *Angew. Chem., Int. Ed.* **2013**, *52* (20), 5280–5284.
- (36) Wang, Q.; Wu, A.; Zhong, S.; Wang, B.; Zhou, R. Highly (h0h)-oriented silicalite-1 membranes for butane isomer separation. *J. Membr. Sci.* **2017**, *540*, 50–59.
- (37) Li, S.; Falconer, J. L.; Noble, R. D. Improved SAPO-34 membranes for CO₂/CH₄ separations. *Adv. Mater.* **2006**, *18* (19), 2601–2603.
- (38) Olson, D. H.; Camblor, M. A.; Villaescusa, L. A.; Kuehl, G. H. Light hydrocarbon sorption properties of pure silica Si-CHA and ITQ-3 and high silica ZSM-58. *Microporous Mesoporous Mater.* **2004**, *67* (1), 27–33.
- (39) Bereciartua, P. J.; Cantín, Á.; Corma, A.; Jordá, J. L.; Palomino, M.; Rey, F.; Valencia, S.; Corcoran, E. W.; Kortunov, P.; Ravikovitch, P. I.; Burton, A.; Yoon, C.; Wang, Y.; Paur, C.; Guzman, J.; Bishop, A. R.; Casty, G. L. Control of zeolite framework flexibility and pore topology for separation of ethane and ethylene. *Science* **2017**, *358*, 1068–1071.
- (40) Avila, A. M.; Funke, H. H.; Zhang, Y.; Falconer, J. L.; Noble, R. D. Concentration polarization in SAPO-34 membranes at high pressures. *J. Membr. Sci.* **2009**, *335* (1), 32–36.
- (41) Keizer, K.; Burggraaf, A. J.; Vroon, Z. A. E. P.; Verweij, H. Two component permeation through thin zeolite MFI membranes. *J. Membr. Sci.* **1998**, *147* (2), 159–172.
- (42) Wang, B.; Gao, F.; Zhang, F.; Xing, W.; Zhou, R. Highly permeable and oriented AlPO-18 membranes prepared using directly synthesized nanosheets for CO₂/CH₄ separation. *J. Mater. Chem. A* **2019**, *7* (21), 13164–13172.
- (43) Mourgues, A.; Sanchez, J. Theoretical analysis of concentration polarization in membrane modules for gas separation with feed inside the hollow-fibers. *J. Membr. Sci.* **2005**, *252* (1), 133–144.
- (44) Chen, W. H.; Lin, C. N.; Chi, Y. H.; Lin, Y. L. Permeation characteristics of hydrogen through palladium membranes in binary and ternary gas mixtures. *Int. J. Energy Res.* **2017**, *41* (11), 1579–1597.
- (45) Himeno, S.; Tomita, T.; Suzuki, K.; Nakayama, K.; Yajima, K.; Yoshida, S. Synthesis and permeation properties of a DDR-type zeolite membrane for separation of CO₂/CH₄ gaseous mixtures. *Ind. Eng. Chem. Res.* **2007**, *46* (21), 6989–6997.
- (46) Robeson, L. M. The upper bound revisited. *J. Membr. Sci.* **2008**, *320* (1), 390–400.
- (47) Zhong, S.; Bu, N.; Zhou, R.; Jin, W.; Yu, M.; Li, S. Aluminophosphate-17 and silicoaluminophosphate-17 membranes for CO₂ separations. *J. Membr. Sci.* **2016**, *520*, 507–514.
- (48) Zhou, Z.; Wu, C.; Zhang, B. ZIF-67 membranes synthesized on α -Al₂O₃-Plate-Supported cobalt nanosheets with amine modification for enhanced H₂/CO₂ permselectivity. *Ind. Eng. Chem. Res.* **2020**, *59* (7), 3182–3188.
- (49) Hillman, F.; Brito, J.; Jeong, H.-K. Rapid One-Pot microwave synthesis of Mixed-Linker hybrid zeolitic-imidazolate framework membranes for tunable gas separations. *ACS Appl. Mater. Interfaces* **2018**, *10* (6), 5586–5593.
- (50) Li, Y.; Ma, C.; Nian, P.; Liu, H.; Zhang, X. Green synthesis of ZIF-8 tubular membranes from a recyclable 2-methylimidazole water-solvent solution by ZnO nanorods self-converted strategy for gas separation. *J. Membr. Sci.* **2019**, *581*, 344–354.
- (51) Al-Maythalony, B. A.; Alloush, A. M.; Faizan, M.; Dafallah, H.; Elgzoly, M. A. A.; Seliman, A. A. A.; Al-Ahmed, A.; Yamani, Z. H.; Habib, M. A. M.; Cordova, K. E.; Yaghi, O. M. Tuning the interplay between selectivity and permeability of ZIF-7 mixed matrix membranes. *ACS Appl. Mater. Interfaces* **2017**, *9* (39), 33401–33407.
- (52) Japip, S.; Xiao, Y.; Chung, T.-S. Particle-Size effects on gas transport properties of 6FDA-Durene/ZIF-71 mixed matrix membranes. *Ind. Eng. Chem. Res.* **2016**, *55* (35), 9507–9517.
- (53) Qian, Q.; Wu, A. X.; Chi, W. S.; Asinger, P. A.; Lin, S.; Hypsher, A.; Smith, Z. P. mixed-matrix membranes formed from imide-functionalized UiO-66-NH₂ for improved interfacial compatibility. *ACS Appl. Mater. Interfaces* **2019**, *11* (34), 31257–31269.